Int. J. Electrochem. Sci., 8 **(2013)** 8940 - 8950

International Journal of
ELECTROCHEMICAL
SCIENCE
www.electrochemsci.org

Electrocatalytic Activity for the Oxygen Reduction on the Novel Carbon Material Containing Nitrogen Prepared by Using Two-Step Pyrolysis of Hemolymph Protein

Chaozhong Guo[1], *Changguo Chen*[1,*], *Zhongli Luo*[2]

[1] Chongqing University, College of Chemistry and Chemical Engineering, Chongqing 400044, China
[2] Chongqing Medical University, College of Basic Medical Sciences, Molecular Medicine and Cancer Research Center, Chongqing 400046, China
[*]E-mail: cgchen@cqu.edu.cn; gcz_2009@hotmail.com

Received: 13 May 2013 / *Accepted:* 5 June 2013 / *Published:* 1 July 2013

There is a growing interest in oxygen electrochemistry as conversions between O_2 and H_2O play an important role in a variety of new energy technologies. Here we design the nitrogen-containing carbon material by using two-step carbonization of hemolymph protein to study the process of oxygen reduction catalysis in alkaline media. The structural and chemical properties of carbon material was studied using the X-ray diffraction, scanning electron microscopy and X-ray photoelectron spectroscopy, and its catalytic activity for the oxygen reduction reaction (ORR), methanol-tolerant performance and long-term stability were evaluated by linear sweeping voltammetry and amperometric *I-t* curve. The results indicate that the ORR onset potential for carbon material is approximately 0.05 V (*vs*. Hg/HgO) being close to the commercial Pt/C catalyst. An important finding is the methanol-tolerant performance and stability of carbon material has outperformed the Pt/C catalyst. We also propose the pyrrolic- and pyridinic-nitrogen groups may be the catalytic active sites for the ORR. This work would stimulate ones to develop the activated carbon materials by using native proteins.

Keywords: Electrocatalysis, Oxygen Reduction, Hemolymph Protein, Pyrolysis, Methanol-Tolerant

1. INTRODUCTION

The ORR cannot only endure a four-electron process to yield water eventually, but also inefficiency two-step, two-electron pathway to form hydrogen peroxide ions as the intermediate [1]. Carbon supported Pt-based catalysts were widely used for ORR electrocatalysis owing to the effective direct four-electron pathway, but the scarcity and high cost of platinum has hindered the commercial applications [2]. Besides, methanol molecule was easy to cross over the proton exchange membrane,

and oxidize on the Pt catalyst resulting in the poor tolerance [3]. Further produced carbon monoxide would also poison the Pt catalyst [3]. Thus, it is urgent to develop inexpensive and efficient ORR catalysts for cost reduction and performance improvement.

Many efforts in the Pt-free electrocatalysts, including polymer coated membranes [4], nitrogen-doped carbon nanotube [5, 6], nitrogen-doped graphene [7], nitrogen-doped carbon aerogels [8] and nitrogen-coordinated nonprecious metal catalysts (NPMCs) [9, 10], have led this area rapidly to development. Especially the NPMCs are considered as the most remarkable substitute for Pt/C catalyst [11-13]. Since Jasinski firstly reported the ORR catalysis of Co phthalocyanine in alkaline environment, various approaches accelerated the development of the NPMCs [14]. Nonprecious metallomacrocyclics, such as iron or cobalt complexes of porphyrin and phthalocyanine and their derivatives, similarly showed the valuable catalysis and considerable promise in ORR, particularly to heat-treatment at elevated temperatures [15-18]. The initial structure of macrocycles was destroyed while some new chemical bonds were formed during the pyrolysis [19, 20]. Remarkably, the pyrolyzed NPMCs were more active and stable than the unpyrolyzed analogues.

Recently, heat-treated carbon materials with heme-containing proteins such as catalase and hemoglobin were proved successful to a Pt-free catalyst, but it was poor in the ORR activity and chemical stability [21-23]. A certain protein, hemin, with heat-treating was also obtained to good ORR catalytic activity [24]. Hemolymph protein (HP) as one of native proteins can be obtained with abundant and inexpensive, and includes a great many complex compounds containing-protoporphyrin. To the best of our knowledge, there is no systematic study on the thermal treatment of HP biomaterial. Therefore, we here use the two-step pyrolysis process coupled with HP to produce heat-treated carbon material, functioning as the ORR-active electrocatalyst. By comparing the commercial Pt/C catalyst, with similar to the onset potential, the long-term stability is superior to the Pt/C catalyst. Our study promotes the rapid development of the ORR-active Pt-free catalyst from native proteins pyrolysis.

2. EXPERIMENTAL PART

2.1. Chemicals and materials

Demic HP was obtained from Chongqing University Hospital and used as received without further purification. Carbon black (Vulcan XC-72R) (VCB) was supplied by Cabot® and pretreated in the solution containing 10% HNO_3 and 30% H_2O_2 at 80℃ for 12 h. All other chemicals were of reagent grade.

2.2. Carbon materials preparation

HP was firstly oven-dried at 100℃ to remove inclusive moisture and then was decomposed in flowing N_2 at 300℃ for 2 h to obtain a precursor. This temperature has been chosen for approaching as close as possible the decomposition temperature of amino acids. The obtained precursor was inserted into a tube furnace for further pyrolysis at 900℃ for 2 h in N_2 atmosphere with a flow rate of 1 L

min^{-1}. After that, the furnace was naturally cooled to the room temperature. For convenience, the obtained catalyst was hereafter named HP300900. In order to explore the influence of metallic species on the ORR catalysis, the HP300900 was treated with 0.5 mol l^{-1} H_2SO_4 solution for 15 h, which was hereafter named HP300900A.

2.3. Physicochemical characterization

Thermogravimetric and differential thermal analysis (TG/DTA) of HP was carried out on a Shimadzu differential thermal analyzer (DTG-60H, Japan) under N_2 flowing. The TG/DTA curves were recorded from room temperature to 600℃ with a ramp rate of 10 ℃ min^{-1}. The X-ray diffraction (XRD) measurements were studied for characterizing the structure of carbon materials using X-ray diffractometer by Shimadzu XRD-6000 (Japan) with Cu $K\alpha_1$ radiation (λ = 1.54178 Å) at the scan rate of 4 °/min. The morphology of carbon materials was characterized by scanning electron microscopy (SEM) on a TESCAN instrument (VEGA 3 LM, Czech Republic) with a high voltage of 20 kV. X-ray photoelectron spectroscopy (XPS) (Thermal Scientific K-Alpha XPS spectrometer) investigated the surface nitrogen groups.

2.4. Electrochemical characterization

Electrochemical measurements, including linear sweeping voltammetry (LSV), cyclic voltammetry (CV) and amperometriy(*I-t* curves) were carried out on a CHI660A electrochemical workstation (CH Instruments, USA) with conventional three-electrode system consisted of a catalytic thin-film working electrode, a ring-shaped Pt wire counter electrode and a standardized Hg/HgO reference electrode. The working electrode was a glassy carbon electrode (GCE, Φ = 5 mm) covered with a thin layer of Nafion-impregnated carbon materials. 10-μl catalyst ink, well-dispersed by 0.5-wt.% Nafion solution/ultrapure water, was dropped onto the GCE surface and then dried at room temperature. The mass loading of carbon materials is ca. 500 μg cm^{-2}. For comparison, the commercial 40-wt.% Pt/C catalyst (purchased from Johnson Matthey Co.) was also investigated and its loading was defined as 250 μg cm^{-2} on the GCE surface.

The basic electrolyte solution was 0.1 mol l^{-1} KOH solution saturated by O_2 or N_2. For the Pt/C catalyst, CVs for the ORR activity were recorded between 0.3 and -0.8 V (*vs.* Hg/HgO) in O_2- or N_2-saturated KOH solution at 5 mV s^{-1}. As to stability experiments, initially stable CV of different catalytic electrode in an O_2-saturated KOH solution was recorded as the first one. And then, a continuous potential cycling of 5000 cycles was performed. After that, CV of different catalytic electrode in an O_2-saturated KOH solution was recorded as the last one. The difference of measurement was that the ORR activity and stability of carbon materials have been evaluated by LSV. LSV were collected by scanning the potential from 0.3 down to -0.7 V at 5 mV s^{-1}. For testing of amperometric *I-t* curves, the working electrodes were applied a potential of -0.10 V with a magnetic stirrer (ca. 600 rpm), and immersed into the electrolyte solution saturated with N_2 over 0 to 300 s,

followed by an immediate introduction of O_2. Afterwards, 5 mol l^{-1} methanol was consecutively added to the O_2-saturated KOH solution at an interval of 200 s.

3. RESULTS AND DISCUSSION

3.1. TG/DTA curves of HP dried powder

Figure 1 shows the result of TG/DTA for HP dried powder. The weight loss of 10% at 150℃ is mainly due to the elimination of H_2O-adsorbed, which causes a board DTA endothermal peak at 75℃. HP began being decomposed at 200℃, and it had been rapidly pyrolyzed with the increment of temperature until approaching to 500℃. The conformation of some irregular endothermal peaks displaying on the DTA curve as well as the weight loss of about 50% on the TGA curve from 200 to 500℃ is mainly attributed to the decomposition of various amino acids contained in this biomaterial. It suggests heat-treated carbonaceous material is a complex mixture. The carbonized procedure of bio-protein accomplished at ~500℃, identical with the TG/DTA result, and the internal structure of low-temperature carbon material changed from the aliphatic carbons to the aromatic carbons [25]. Here we have preferred 200, 300, 350, 400 and 500℃ as the first-step pyrolysis temperature to produce the HP pyropolymer, which is an intermediate substance between a polymer and heat-treated carbon material [23]. These pyropolymers were applied to function as the catalyst precursors, and the activated carbon material with the highest catalytic activity was obtained by using the pyropolymer formation at 300℃ as the optimal precursor.

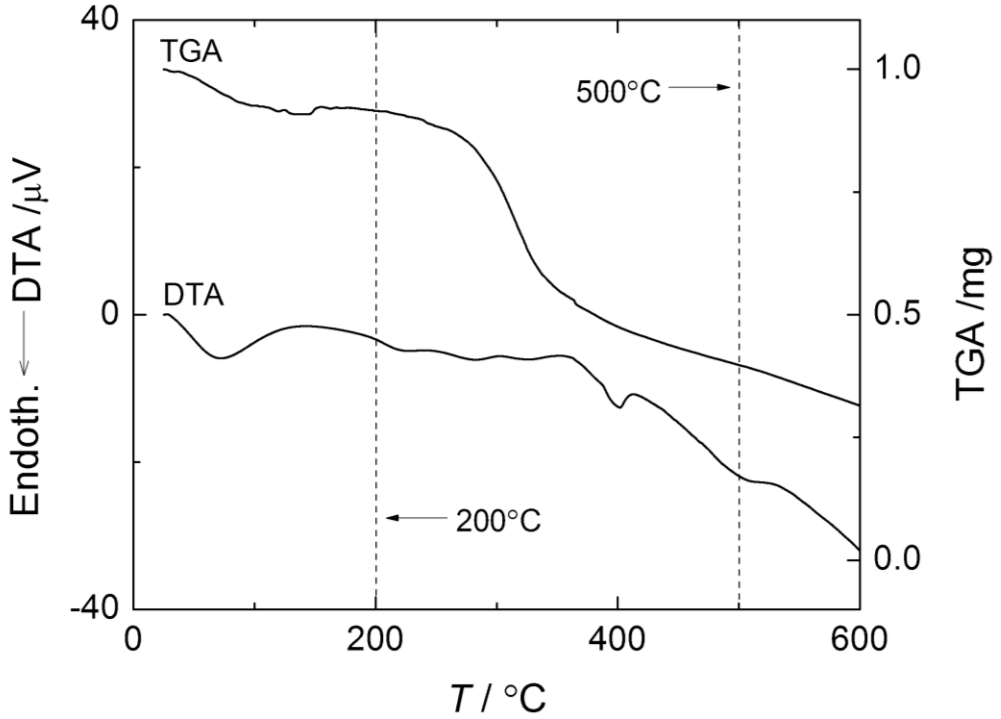

Figure 1. The TG/DTA curves of the HP dried powder

3.2. Electrocatalytic behavior of carbon materials toward ORR

Figure 2a shows the LSV curves of VCB, HP300900 and HP300900A in 0.1 mol l^{-1} KOH solution saturated by N_2 or O_2. The onset potential, peak potential and peak current was used as the parameters of evaluating electrochemical catalytic activity of carbon materials. The VCB displays the electrocatalytic activity toward ORR in alkaline media, but possesses a negative onset potential and a weak cathodic peak with a small peak current.

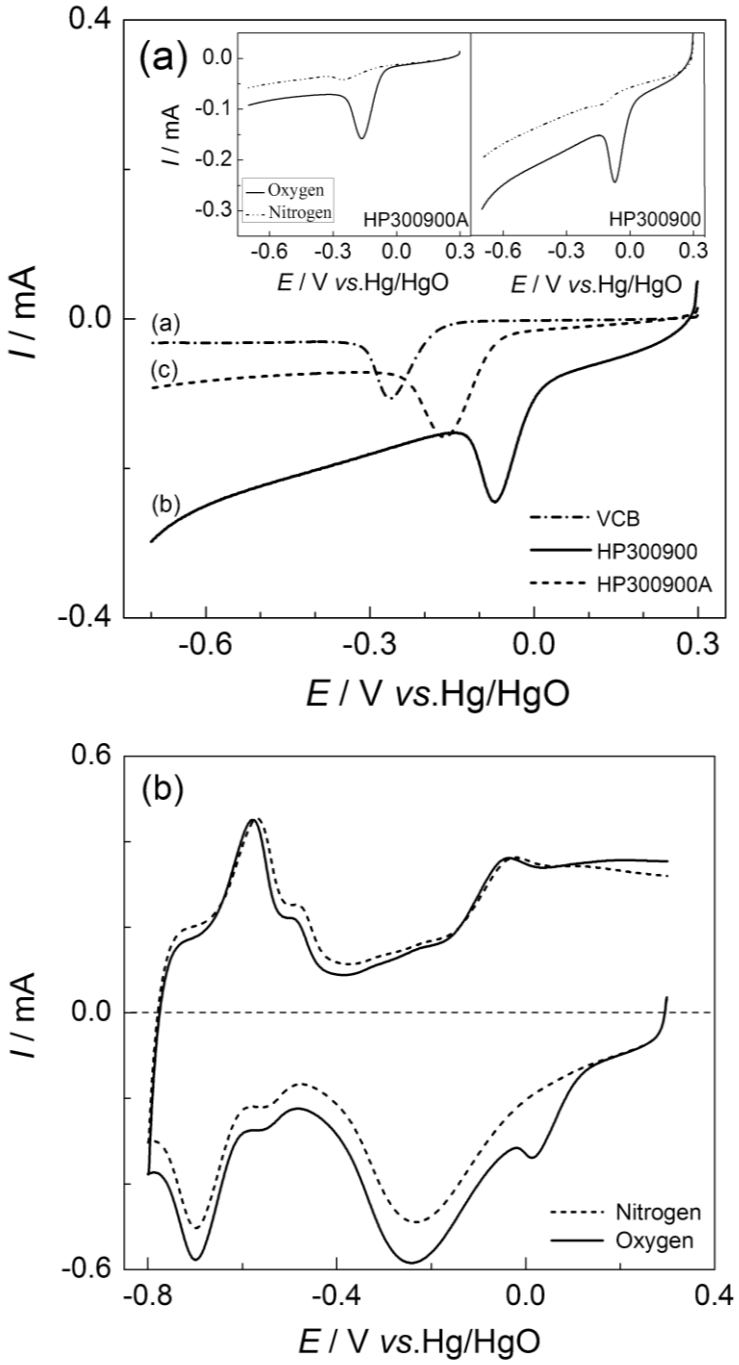

Figure 2. (**a**) LSVs of VCB (a), HP300900 (b) and HP300900A (c) in 0.1 mol l^{-1} KOH solution saturated by O_2; (**b**) CVs of Pt/C catalyst in 0.1 mol l^{-1} KOH solution saturated by O_2 and N_2.

The heat-treated carbon material from HP pyrolysis exhibits better ORR electrocatalysis with an onset potential of 0.05 V (*vs.* Hg/HgO) and a cathodic peak potential of -0.07 V, and its ORR peak current increases about one and a half times (comparing with that of VCB). By comparing the Pt/C catalyst with the HP300900, it can be found that they have similar onset potentials for ORR, even though the cathodic peak current of Pt/C is larger than the latter (Figure 2b). It shows the HP300900 material has an excellent electrocatalytic activity toward ORR. In addition, the hydrogen adsorption and desorption peaks of the Pt/C catalyst are almost maintained regardless of the presence of oxygen or nitrogen. The acid-treated material HP300900A also exhibits a good ORR activity, but its ORR onset potential has slightly moved (ca. 70 mV) to a more negative potential (Fig. 2a). A reasonable elucidation is a trace of metallic species in this carbon material is further reduced by the acid-treatment, which has been checked by elemental microanalysis (not shown here). However, the decrease of metallic species has limitedly affected the ORR catalytic activity of carbon material. Thus, we propose that the metallic species is not a prerequisite to the ORR-active site, and yet may be used to improve the catalytic activity of carbon material, which are in accordance with the previously reported results [26, 27].

3.3. XRD, SEM and XPS analysis of carbon materials

Figure 3a and 3b are the SEM images of HP300900 and HP300900A. The particle-size of carbon material in micrometer has reduced to a smaller size owing to the acid-treatment. This treatment may cause more ORR-active sites to expose on the surface of carbon material [27].

The XRD patterns of carbon material before and after leaching in an acidic solution are shown in Figure 3c. For both materials, no other peaks are evidently observed in the XRD patterns except for two board diffraction peaks including a large broad peak at $2\theta = 25^{\circ}$ (graphite 002) and a small broad peak at $2\theta = 44^{\circ}$ (graphite 101). From the XRD pattern of VCB, these peaks are associated with amorphous carbon, usually remarked for activated carbon [28]. Compared to the carbon black (VCB), two diffraction peaks have become wider and shifted slightly, which may be caused by formation of C-N bonding groups and lower graphitization degree. This result can provide little information for nitrogen doped into the carbon structure.

Figure 3d shows the XPS spectra of N1s region to HP300900 and HP300900A. Both carbon materials exhibit three nitrogen groups, including the pyridinic-N (ca. 398.3 eV), pyrrolic-N (ca. 399.9 eV) and graphitic-N groups (ca. 401.4 eV) [29-31]. These types of nitrogen were often obtained to the carbonization of nitrogen-containing organics [32, 33]. Additionally, after acid-treatment of HP300900, the relative intensity of nitrogen groups has increased. An elucidation is an addition of total nitrogen content including in the HP300900A resulted from several metallic species losing. Compared to the pyridinic-N and graphitic-N groups (Table 1), the carbon materials have a larger fraction of the pyrrolic-N group, mainly responsible for ORR catalysis. Increasing the acid-treatment for HP300900 mainly transforms pyridinic-N to pyrrolic-N group, which could generate the limited difference of catalytic activity between HP300900 and HP300900A. It indicates the pyrrolic-N and pyridinic-N groups may be the active sites for ORR.

Table 1. XPS: N1s binding energies and relative contents of the carbon materials.

Sample	Pyridinic-N		Pyrrolic-N		Graphitic-N	
	B.E. / eV	at.%	B.E. / eV	at.%	B.E. / eV	at.%
HP300900	398.3	32.4	399.9	44.6	401.4	23.0
HP300900A	398.5	29.4	400.0	47.1	401.4	23.5

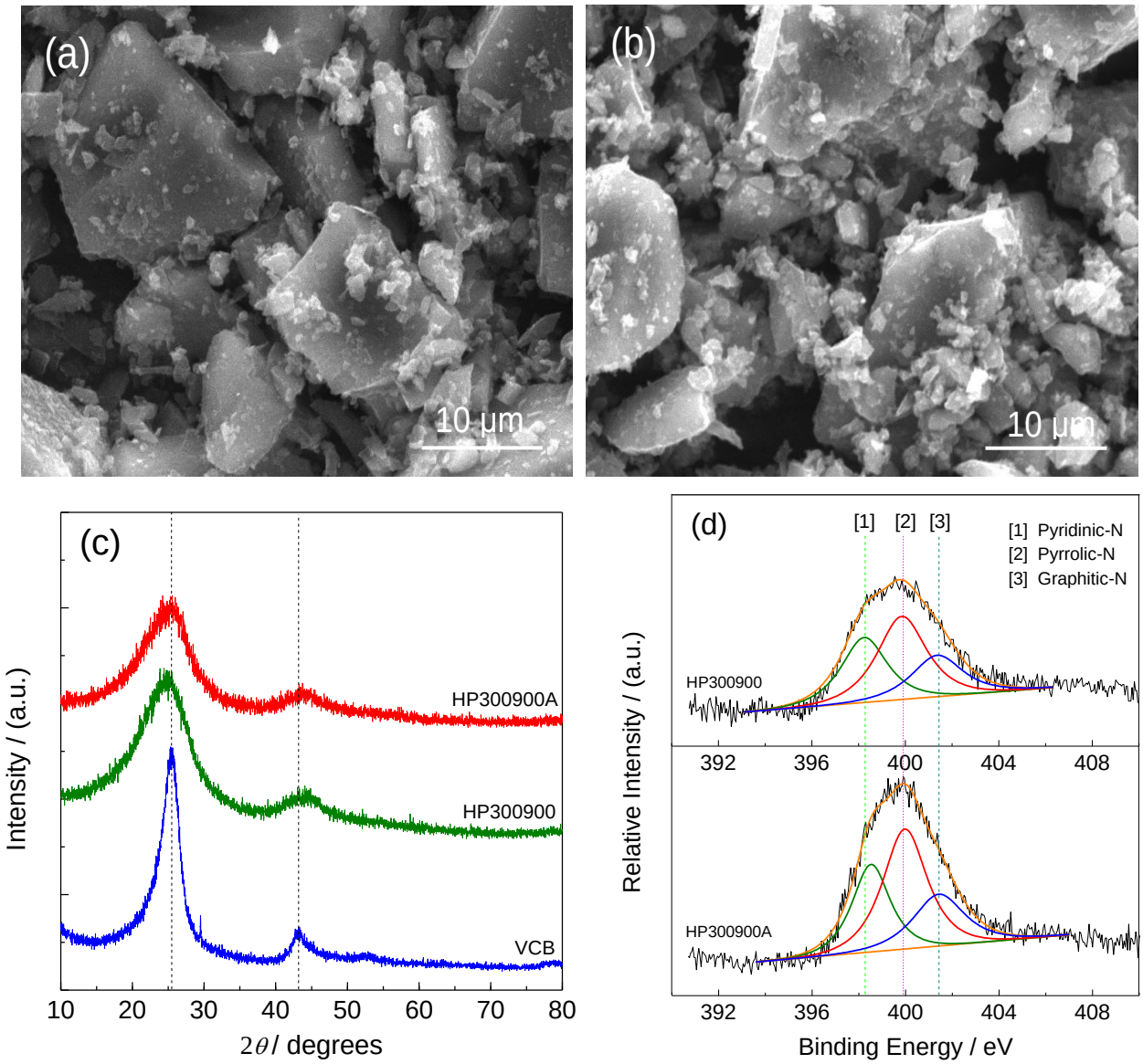

Figure 3. (**a**) SEM image of HP300900; (**b**) SEM image of HP300900A; (**c**) XRD patterns of HP300900, HP300900A and VCB; (**d**) XPS spectra of N1s region obtained for the HP300900 and HP300900A.

3.4. Methanol-tolerant properties and stability of carbon materials

The HP300900 has the excellent electrocatalytic activity with a positive onset potential for ORR, indicating a potential to replace the commercial Pt-based catalysts. However, better methanol-

tolerant property and long-term stability are essential to rapidly achieve practical commercialization. Therefore, chronoamperometric method was used to check the electrocatalytic specificity of catalytic electrodes coated with carbon materials against the electro-oxidation of methanol. The *I-t* chronoamperometric responses of carbon materials are shown in Figure 4a, which demonstrates a step-down decrease in cathodic current response upon the successive addition of 5.0 mol l^{-1} methanol.

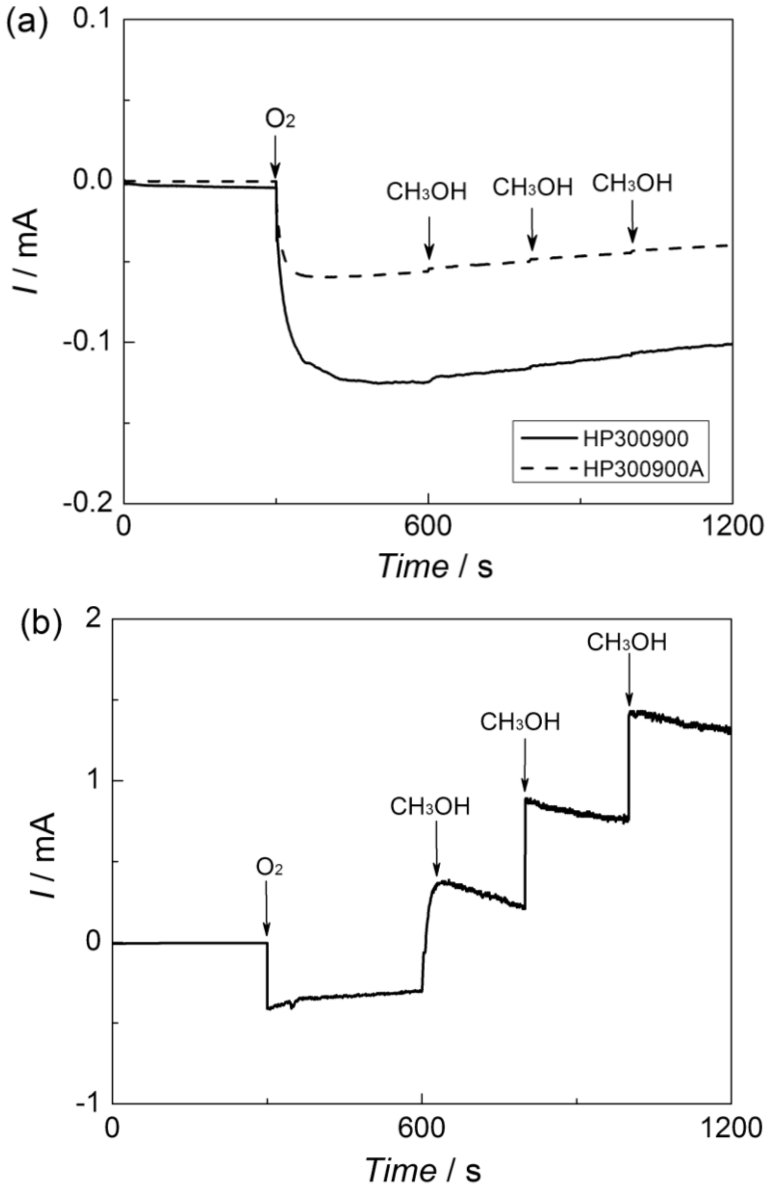

Figure 4. (**a**) Amperometric *I-t* curves obtained at HP300900 (bold line) and HP300900A (dash line) in N_2-saturated 0.1 mol l^{-1} KOH solution under magnetic stirring (600 rpm) and N_2-protection over 0 to 300 s, followed by an immediate introduction of O_2. The applied potential is -0.1 V and arrows indicate the sequential addition of 5.0 mol l^{-1} methanol. (**b**) Amperometric *I-t* curves obtained at the Pt/C catalyst. Other conditions are identical to Fig.4(a).

The stable amperometric response for the ORR remained fairly balanced tendency while the sequential addition of the methanol solution was performed at the time interval of 200 s. These results confirm the electro-oxidation of methanol on the HP300900 catalytic electrode is sluggish. The similar

result is also obtained for HP300900A in addition of lower amperometric response to ORR than that of HP300900.

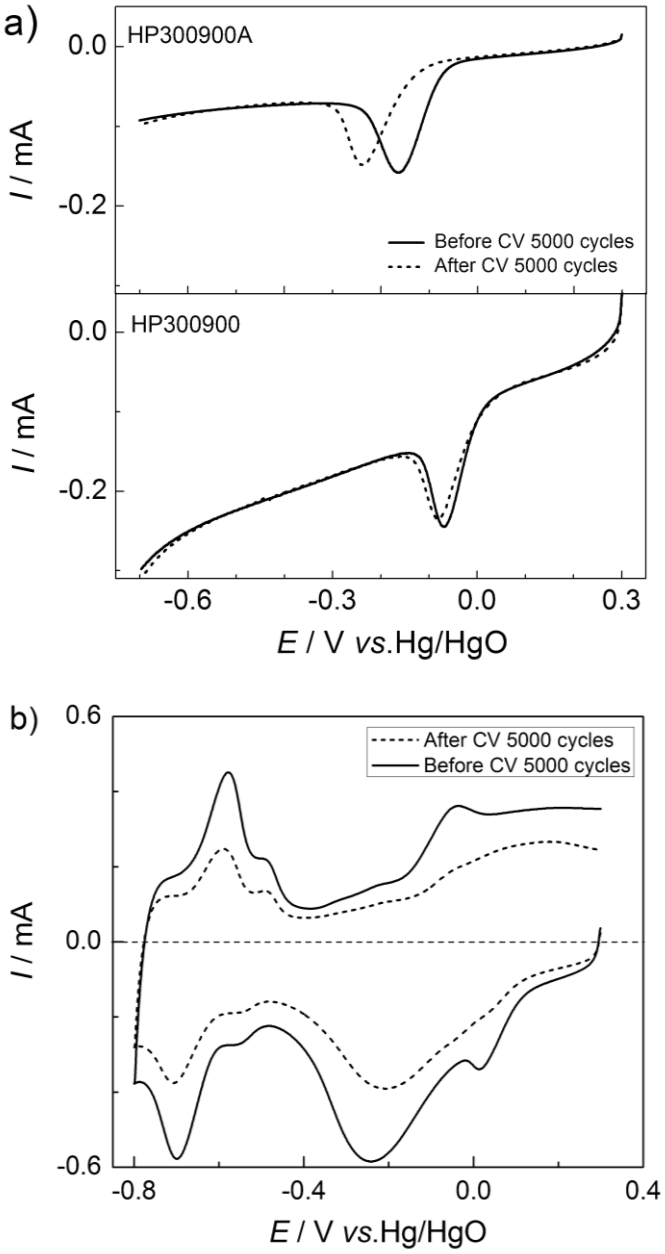

Figure 5. (**a**) LSVs of HP300900 and HP300900A before (bold line) and after (dash line) a continuous potential cycling for 5000 in O_2-saturated 0.1 mol l^{-1} KOH solution; (**b**) CVs of the Pt/C catalyst before (bold line) and after (dash line) a successive potential cycling for 5000 in O_2-saturated KOH solution

To better understand the remarkable methanol-tolerant performance of carbon materials, the commercial Pt/C catalyst was investigated further in Figure 4b. The methanol is too convenient for electro-oxidation at the Pt/C catalyst, leading to losing its ORR activity absolutely. Meanwhile, a step-down increase in the current response upon the successive addition of 5.0 mol l^{-1} methanol is also observed. Such excellent specificity toward ORR and notable methanol-tolerant behavior could be

attributable to much lower ORR potential on this carbon material than that required for electro-oxidation of methanol. To explore the long-term stability of both HP300900 and HP300900A toward ORR in alkaline media, the potential was continuously cycled between 0.3 and -0.7 V for HP300900 and HP300900A in O_2-saturated 0.1 mol l^{-1} KOH for 5000 cycles. The rapid degeneration of HP300900A catalytic electrode has happened, and its onset potential and the peak potential for ORR have kept away from the initial curve (Figure 5a). The catalytic electrode coated with HP300900 has shown almost equivalent voltammetric responses before and after the cycling sweep under the same condition, which suggests that the HP300900 is extraordinarily stable during the aging-resistance testing. The large difference of stability may be due to the acid-treatment, which implies that the metallic species in the carbon material has also played a critical role in maintaining the stability toward ORR. Thus, it can be concluded that the reduction of metallic species can not only influence the ORR activity, but also damages the long-term stability of this carbon material. For comparison, the stability of the Pt/C catalyst for ORR electrocatalysis has been studied. As shown in Figure 5b, the sharp deterioration of Pt occurs on the commercial Pt/C catalytic electrode, suggesting the HP300900 catalytic electrode has a much higher stability than the Pt/C catalytic electrode. The reasons may be as follows. a) The nature of nitrogen-doped active sites is different from Pt-based catalysts [34, 35]. b) The successive potential cycling might cause the migration or aggregation of Pt nanoparticles and subsequent loss of the ORR catalytic activity [36].

4. CONCLUSIONS

Here we report the preparation and electrochemical oxygen reduction activity of the novel carbon material containing-nitrogen from two-step pyrolysis of HP biomaterial. The results show that the HP pyropolymer formed at 300℃ is the most suitable for fabricating the ORR-active catalyst, which yields comparable electrocatalytic activity to the commercial Pt/C catalyst while heat-treated at 900℃. The ORR onset potentials for the carbon material and Pt/C catalyst are substantially similar (ca. 0.05 V *vs.* Hg/HgO). An interesting finding is the methanol-tolerant performance and stability of carbon material has priority to the Pt/C catalyst. We also propose the pyrrolic-N and pyridinic-N groups may be the active sites for ORR. The metallic species are not a prerequisite for forming the ORR-active sites based on that the acid-treated carbon material has remained the excellent ORR activity. However, the mechanism for ORR on this carbon material containing-nitrogen will need further study.

ACKNOWLEDGEMENTS
This work was supported by Natural Science Fund of China (Project No. 21273292) and the Fundamental Research Funds for the Central Universities (Project No. CDJXS12220002). We thank Yujun Si, Wei Yin, Ping Liu and Mo Du for their helpful discussion.

References

1. L. Carrette, K. A. Friedrich and U. Stimming, *ChemPhysChem*, 1 (2000) 162.
2. S. C. Thomas, X. M. Ren, S. Gottesfeld and P. Zelenay, *Electrochim. Acta*, 47 (2002) 3741.
3. D. J. Ham, Y. K. Kim, S. H. Han and J. S. Lee, *Catal. Today* 132 (2008) 117.

4. B. Winther-Jensen, O. Winther-Jensen, M. Forsyth and D. R. MacFarlane, *Science*, 321 (2008) 671.
5. Z. Y. Mo, S. J. Liao, Y. Y. Zheng and Z. Y. Fu, *Carbon*, 50 (2012) 2620.
6. N. Alexeyeva, E. Shulga, V. Kisand, I. Kink and K. Tammeveski, *J. Electroanal. Chem.*, 648 (2010) 169.
7. S. Y. Yang, K. H. Chang, Y. L. Huang, Y. F. Lee, H. W. Tien, S. M. Li, Y. H. Lee, C. H. Liu, C. C. M. Ma and C. C. Hu, *Electrochem. Commun.*, 14 (2012) 39.
8. Y. Wei, S. Z. Chen and W. M. Lin, *Int. J. Hydrogen Energ*., 37 (2012) 942.
9. M. Lefèvre, E. Proietti, F. Jaouen and J. P. Dodelet, *Science*, 324 (2009) 71.
10. X. X. Yuan, X. Zeng, H. J. Zhang, Z. F. Ma and C. Y. Wang, *J. Am. Chem. Soc*., 132 (2010) 1754.
11. T. Yang and G. Q. Han, *Int. J. Electrochem. Sci*., 7 (2012) 10884.
12. C. W. B. Bezerra, L. Zhang, H. S. Liu, K. C. Lee, A. L. B. Marques, E. P. Marques, H. J. Wang and J. J. Zhang, *J. Power Sources*, 173 (2007) 891.
13. N. A. Karima and S. K. Kamarudin, *Appl. Energ*., 103 (2013) 212.
14. R. Jasinski, *Nature*, 201 (1964) 1212.
15. X. F. Dai, J. L. Qiao, X. J. Zhou, J. J. Shi, P. Xu, L. Zhang and J. J. Zhang, *Int. J. Electrochem. Sci.*, 8 (2013) 3160.
16. C. W. B. Bezerra, L. Zhang, K. C. Lee, H. S. Liu, A. L. B. Marques, E. P. Marques, H. J. Wang and J. J. Zhang, *Electrochim. Acta*, 53 (2008) 4937.
17. J. H. Zagal, F. Bedioui and J. P. Dodelet, N_4-Macrocyclic Metal Complexes, Springer, New York (2006).
18. I. Kruusenberg, L. Matisen, Q. Shah, A. M. Kannan and K. Tammeveski, *Int. J. Hydrogen Energ*., 37 (2012) 4406.
19. S. Gupta, D. Tryk, I. Bae, W. Aldred and E. Yeager, *J. Appl. Electrochem*., 19 (1989) 19.
20. L. Zhang, J. J. Zhang, D. P. Wilkinson and H. J. Wang, *J. Power Sources*, 156 (2006) 171.
21. M. E. Lai and A. Bergel, *J. Electroanal. Chem*., 494 (2000) 30.
22. J. Maruyama and I. Abe, *Chem. Mater*., 18 (2006) 1303.
23. J. Maruyama, J. J. Okamura, K. Miyazaki and I. Abe, *J. Phys. Chem*. C, 111 (2007) 6597.
24. Z. X. Liang, H. Y. Song and S. J. Liao, *J. Phys. Chem*. C, 115 (2011) 2604.
25. J. Maruyama, J. J. Okamura, K. Miyazaki, Y. Uchimoto and I. Abe, *J. Phys. Chem*. C, 112 (2008) 2784.
26. Y. J. Si, C. G. Chen, W. Yin and H. Cai, *Chin. Chem. Lett*., 21 (2010) 983.
27. Y. J. Si, C. G. Chen, W. Yin and H. Cai, *Chin. J. Chem. Phys*., 23 (2010) 331.
28. M. Bron, J. Radnik, M. Fieber-Erdmann, P. Bogdanoff and S. Fiechter, *J. Electroanal. Chem*., 535 (2002) 113.
29. K. Stanczyk, R. Dziembaj, Z. Piwowarska and S. Witkowski, *Carbon*, 33 (1995) 1383.
30. R. J. J. Jansen and H. van Bekkum, *Carbon*, 33 (1995) 1021.
31. J. Casanovas, J. M. Ricart, J. Rubio, F. Illas and J. M. Jimenez-Mateos, *J. Am. Chem. Soc*., 118 (1996) 8071.
32. J. R. Pels, F. Kapteijn, J. A. Moulijin, Q. Zhu and K. M. Thomas, *Carbon*, 33 (1995) 1641.
33. H. Schmiers, J. Friebel, P. Streubel, R. Hesse and R. Köpsel, *Carbon*, 37 (1999) 1965.
34. P. H. Matter and U. S. Ozkan, *Catal. Lett*., 109 (2006) 115.
35. Y. M. Yu , J. H. Zhang, C. H. Xiao, J. D. Zhong, X. H. Zhang and J. H. Chen, *Fuel Cells*, 12 (2012) 506.
36. G. Q. Mo, S. Y. Liao, Y. Z. Zhang, W. D. Zhang and J. S. Ye, *Electrochim. Acta*, 76 (2012) 430.

© 2013 by ESG (www.electrochemsci.org)